Proceedings of the American Control Conference
San Diego, California • June 1999

Adaptive Robust Motion Control Of Single-Rod Hydraulic Actuators: Theory and Experiments

Bin Yao + Fanping Bu John Reedy George T. C. Chiu

School of Mechanical Engineering
Purdue University, West Lafayette, IN 47906, USA
+ Email: *byao@ecn.purdue.edu*

Abstract

High performance robust motion control of single-rod hydraulic actuators is considered. In contrast to the double-rod hydraulic actuators studied previously, the two chambers of a single-rod hydraulic actuator have different areas. As a result, the dynamic equations describing the pressure changes in the two chambers cannot be combined into a single load pressure equation. This complicates the controller design since it not only increases the dimension of the system to be dealt with but also brings in the stability issue of the added internal dynamics. A discontinuous projection based adaptive robust controller is constructed. The controller is able to take into account not only the effect of parameter variations coming from the inertia load and various hydraulic parameters but also the effect of hard-to-model nonlinearities such as uncompensated friction forces and external disturbances. Extensive experimental results are obtained for the swing motion control of a hydraulic arm. In comparison to a state-of-the-art industrial motion controller, the proposed ARC algorithm achieves more than a magnitude reduction of tracking errors. Furthermore, during constant velocity and regulation periods, the ARC controller reduces the tracking errors almost down to the measurement resolution level.

1 Introduction

The dynamics of hydraulic systems are highly nonlinear [1]. Furthermore, the system may be subjected to non-smooth and discontinuous nonlinearities due to control input saturation, directional change of valve opening, friction, and valve overlap. Aside from the nonlinear nature of hydraulic dynamics, hydraulic systems also have large extent of model uncertainties such as the large changes of load and the hydraulic parameters (e.g., bulk modulus), the external disturbances, leakage flows, and friction. In the past, much of the work in the control of hydraulic systems uses linear control theory [2, 3, 4, 5] and feedback linearization techniques [6, 7]. In [8], Alleyne and Hedrick applied the nonlinear adaptive control to the force control of an active suspension driven by a double-rod cylinder, in which only parametric uncertainties of the cylinder are considered.

In [9], the adaptive robust control (ARC) approach proposed by Yao and Tomizuka in [10, 11] was generalized to provide a rigorous theoretic framework for the high performance robust control of a double-rod electro-hydraulic servo-system by taking into account the particular nonlinearities and model uncertainties of the electro-hydraulic servo-systems. The presented ARC scheme uses smooth projections [12] to solve the design conflicts between adaptive control design and robust control design, which is technical and may not be convenient for practical implementation. In [13], the recently proposed discontinuous projection based ARC design [11] is generalized to solve the practical problems associated with smooth projections [9].

This paper continues the work done in [13] and will generalize the results to the electro-hydraulic systems driven by single-rod actuators. To test the proposed advanced nonlinear ARC strategy, a three-link robot arm (a scaled down version of excavator arm) driven by three hydraulic cylinders has been set up. Extensive comparative experimental results have been obtained for the swing motion control of the hydraulic arm. Experimental experience and results are provided to illustrate the proposed method.

2 Problem Formulation and Dynamic Models

The system under consideration is the same as that in [9, 13] but with a single-rod hydraulic cylinder, which is depicted in Fig. 1. The goal is to have the inertia load to track any specified motion trajectory as closely as possible; examples like a machine tool axis [14].

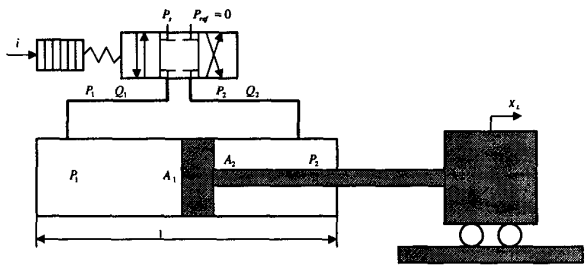

Figure 1: Single-Rod Electro-Hydraulic Servo Systems

The dynamics of the inertia load can be described by

$$m\ddot{x}_L = P_1 A_1 - P_2 A_2 - b\dot{x}_L - F_{fc}(\dot{x}_L) + \tilde{f} \qquad (1)$$

where x_L and m represent the displacement and the mass of the load respectively, P_1 and P_2 are the pressures inside the two chambers of the cylinder, A_1 and A_2 are the ram areas of the two chambers, b represents the combined coefficient of the modeled damping and viscous friction forces on the load and the cylinder rod, F_{fc} represents the modeled Coulomb friction force, and $\tilde{f}(t, x_L, \dot{x}_L)$ represents the lumped uncertain nonlinearities due to external disturbances, the unmodeled friction forces, and other unmodeled terms. The actuator (or the cylinder) dynamics can be written as [1]:

$$\begin{aligned} \frac{V_1}{\beta_e}\dot{P}_1 &= -A_1\dot{x}_L - C_{tm}(P_1 - P_2) - C_{em1}(P_1 - P_r) + Q_1 \\ \frac{V_2}{\beta_e}\dot{P}_2 &= A_2\dot{x}_L + C_{tm}(P_1 - P_2) - C_{em2}(P_2 - P_r) - Q_2 \end{aligned} \tag{2}$$

where $V_1 = V_{h_1} + A_1 x_L$ and $V_2 = V_{h_2} - A_2 x_L$ are the total control volumes of the two chambers respectively, V_{h1} and V_{h2} are the two chamber volumes when $x_L = 0$,β_e is the effective bulk modulus, C_{tm} is the coefficient of the internal leakage of the cylinder, C_{em1} and C_{em2} are the coefficients of the external leakage of the two chambers respectively, Q_1 is the supplied flow rate to the forward (or cylinder-end) chamber, and Q_2 is the return flow rate of the return (or rod-end) chamber. By re-defining the reference position for x_L if necessary, $V_{h1} = V_{h2} = V_h$, which is assumed in this paper for simplicity. Q_1 and Q_2 are related to the spool valve displacement of the servovalve, x_v, by [1]

$$\begin{aligned} Q_1 &= k_{q1}x_v\sqrt{\Delta P_1}, \quad \Delta P_1 = \begin{cases} P_s - P_1 & \text{for} \quad x_v \geq 0 \\ P_1 - P_r & \quad\quad x_v < 0 \end{cases} \\ Q_2 &= k_{q2}x_v\sqrt{\Delta P_2}, \quad \Delta P_2 = \begin{cases} P_2 - P_r & \text{for} \quad x_v \geq 0 \\ P_s - P_2 & \quad\quad x_v < 0 \end{cases} \end{aligned} \tag{3}$$

where k_{q1} and k_{q2} are the flow gain coefficients of the servo valve, P_s is the supply pressure of the fluid, and P_r is the tank or reference pressure. For simplicity, in this study, the valve dynamics is neglected and x_v will be treated as the control input; if states of the valve dynamics are measurable, the same strategy as in [9, 13] can be used to handle the additional valve dynamics if necessary.

As in [13], to minimize the numerical error and facilitate the gain-tuning process, scaling factors are introduced to the pressures and the valve opening as $\bar{P}_1 = \frac{1}{S_{c3}}P_1$, $\bar{P}_2 = \frac{1}{S_{c3}}P_2$, $\bar{P}_s = \frac{1}{S_{c3}}P_s$, $\bar{P}_r = \frac{1}{S_{c3}}P_r$, and $\bar{x}_v = \frac{1}{S_{c4}}x_v$, where S_{c3} and S_{c4} are constant scaling factors. Define the state variables $x = [x_1, x_2, x_3, x_4]^T \triangleq [x_L, \dot{x}_L, \bar{P}_1, \bar{P}_2]^T$, the entire system, Eqs.(1) to (3) can be expressed in state space form as

$$\begin{aligned} \dot{x}_1 &= x_2 \\ \dot{x}_2 &= \tfrac{S_{c3}A_1}{m}(x_3 - \bar{A}_c x_4 - \bar{b}x_2 - \bar{F}_{fc}(x_2)) + d(x_1, x_2, t) \\ \dot{x}_3 &= h_1(x_1)\left[\tfrac{\beta_e S_{c4}k_{q1}}{\sqrt{S_{c3}V_h}}\left(-\bar{A}_1 x_2 + g_3(x_3, sign(u))u\right)\right. \\ &\quad \left. - \tfrac{C_{tm}\beta_e}{V_h}(x_3 - x_4) - \tfrac{C_{em1}\beta_e}{V_h}(x_3 - \bar{P}_r)\right] \\ \dot{x}_4 &= h_2(x_1)\left[\tfrac{\beta_e S_{c4}k_{q1}}{\sqrt{S_{c3}V_h}}\left(\bar{A}_2 x_2 - g_4(x_4, sign(u))u\right)\right. \\ &\quad \left. + \tfrac{C_{tm}\beta_e}{V_h}(x_3 - x_4) - \tfrac{C_{em2}\beta_e}{V_h}(x_4 - \bar{P}_r)\right] \end{aligned} \tag{4}$$

where $\bar{A}_c = \frac{A_2}{A_1}$, $\bar{b} = \frac{b}{S_{c3}A_1}$, $\bar{F}_{fc} = \frac{F_{fc}(\dot{x}_L)}{S_{c3}A_1}$, $d = \frac{1}{m}\tilde{f}(t, x_L, \dot{x}_L)$, $h_1(x_1) = \frac{1}{1+\bar{A}_{h1}x_1}$, $h_2(x_1) = \frac{1}{1-\bar{A}_{h2}x_1}$, $\bar{A}_{h1} = \frac{A_1}{V_h}$, $\bar{A}_{h2} = \frac{A_2}{V_h}$, $\bar{A}_1 = \frac{A_1}{k_{q1}S_{c4}\sqrt{S_{c3}}}$, $\bar{A}_2 = \frac{A_2}{k_{q1}S_{c4}\sqrt{S_{c3}}}$, $u = \bar{x}_v$ is the control input, and g_3 and g_4 are defined by

$$\begin{aligned} g_3 &= \sqrt{\overline{\Delta P_1}}, \quad \overline{\Delta P_1} = \tfrac{1}{S_{c3}}\Delta P_1(x_3, sign(u)) \\ g_4 &= k_{qc}\sqrt{\overline{\Delta P_2}}, \quad \overline{\Delta P_2} = \tfrac{1}{S_{c3}}\Delta P_2(x_4, sign(u)) \end{aligned} \tag{5}$$

in which $k_{qc} = \frac{k_{q2}}{k_{q1}}$.

Given the desired motion trajectory $x_{Ld}(t)$, the objective is to synthesize a control input u such that the output $y = x_1$ tracks $x_{Ld}(t)$ as closely as possible in spite of various model uncertainties.

3 Discontinuous Projection Based ARC

In this paper, we only consider the parametric uncertainties due to m, β_e, the nominal value of the disturbance d, d_n, leakage coefficients C_{tm}, C_{em1}, and C_{em2}. Define the unknown parameter set $\theta = [\theta_1, \theta_2, \theta_3, \theta_4, \theta_5, \theta_6]^T$ as $\theta_1 = \frac{S_{c3}A_1}{m}$, $\theta_2 = d_n$, $\theta_3 = \frac{\beta_e S_{c4}k_{q1}}{V_h\sqrt{S_{c3}}}$, $\theta_4 = \frac{C_{tm}\beta_e}{V_h}$, $\theta_5 = \frac{C_{em1}\beta_e}{V_h}$, $\theta_6 = \frac{C_{em2}\beta_e}{V_h}$. The state space equation (4) can be linearly parametrized in terms of θ as

$$\begin{aligned} \dot{x}_1 &= x_2 \\ \dot{x}_2 &= \theta_1(x_3 - \bar{A}_c x_4 - \bar{b}x_2 - \bar{F}_{fc}(x_2)) + \theta_2 + \tilde{d}(t, x_1, x_2) \\ \dot{x}_3 &= h_1\left[\theta_3(-\bar{A}_1 x_2 + g_3 u) - \theta_4(x_3 - x_4) - \theta_5(x_3 - \bar{P}_r)\right] \\ \dot{x}_4 &= h_2\left[\theta_3(\bar{A}_2 x_2 - g_4 u) + \theta_4(x_3 - x_4) - \theta_6(x_4 - \bar{P}_r)\right] \end{aligned} \tag{6}$$

where $\tilde{d} = d - d_n$. As in [9, 13], it is assumed that

$$\begin{aligned} \theta &\in \Omega_\theta \triangleq \{\theta : \ \theta_{min} < \theta < \theta_{max}\} \\ |\tilde{d}| &\leq \delta_d(x_1, x_2, t) \end{aligned} \tag{7}$$

where $\theta_{min} = [\theta_{1min}, \ldots, \theta_{6min}]^T$, $\theta_{max} = [\theta_{1max}, \ldots, \theta_{3max}]^T$ and $\delta_d(t, x_1, x_2)$ are known. Physically, $\theta_1 > 0$ and $\theta_3 > 0$. So it is assumed that $\theta_{1min} > 0$ and $\theta_{3min} > 0$.

At this stage, it is ready to see that the main difficulties in controlling (6) are: (i) the system has unmatched model uncertainties since parametric uncertainties and uncertain nonlinearities appear in equations that do not contain control input u; this difficult can be overcome by employing backstepping ARC design as done in the following; (ii) the nonlinear static flow gains g_3 and g_4 are functions of u also and are *non-smooth* ; (iii) as will become clear later, the "relative degree" of the system is three. Since the system state has a dimension of four, there will exist a one-dimensional internal dynamics after an ARC controller is synthesized via backstepping. It is thus necessary to check the stability of the resulting internal dynamics.

In the following, the discontinuous projection based ARC design for double-rod hydraulic cylinders [13] will be generalized to overcome the first two difficulties to obtain an ARC controller for (6). Due to space limit, only outline of the controller design is given. The detailed design procedures and stability proofs can be obtained from the authors and/or worked out using similar techniques as in [13].

Let $\hat{\theta}$ denote the estimate of θ and $\tilde{\theta}$ the estimation error (i.e., $\tilde{\theta} = \hat{\theta} - \theta$). The following adaptation law structure will be sought

$$\dot{\hat{\theta}} = Proj_{\hat{\theta}}(\Gamma\tau) \tag{8}$$

where $\Gamma > 0$ is a diagonal matrix, τ is an adaptation function to be synthesized later, and $Proj_{\hat{\theta}}(\bullet)$ is the widely used discontinuous projection mapping [10]. For simplicity, let $\hat{\dot{x}}_2$ represent the calculable part of the $\dot{x}_2$ given by

$$\hat{\dot{x}}_2 = \hat{\theta}_1(x_3 - \bar{A}_c x_4 - \bar{b}x_2 - \bar{F}_{fc}(x_2)) + \hat{\theta}_2 \qquad (9)$$

ARC Controller Design

The design parallels the recursive backstepping ARC design in [11, 13] as follows.

Step 1

Define $P_L = x_3 - \bar{A}_c x_4$. It is seen from (6) that P_L can be thought as the input to the first two equations of (6). Furthermore, the resulting two equations have the same form as those in [13]. Thus, the same ARC design technique can be used to construct an ARC control function $\alpha_2(x_1, x_2, \hat{\theta}_1, \hat{\theta}_2, t)$ for the virtual control input P_L such that the output tracking error $e_1 = x_1 - x_{1d}(t)$ converges to zero or a small value with a guaranteed transient performance. The resulting control function α_2 and adaptation function $\tau_2(x_1, x_2, \hat{\theta}_1, \hat{\theta}_2, t)$ are given by

$$\begin{aligned}
&\alpha_2 = \alpha_{2a} + \alpha_{2s} \\
&\quad \alpha_{2a} = \bar{b}x_2 + \bar{F}_{fc} + \tfrac{1}{\hat{\theta}_1}(\dot{x}_{2eq} - \hat{\theta}_2) \\
&\quad \alpha_{2s} = \alpha_{2s1} + \alpha_{2s2} \\
&\quad \alpha_{2s1} = -\tfrac{1}{\theta_{1min}} k_{2s1} z_2, \quad k_{2s1} \geq \|C_{\phi 2}\Gamma\phi_2\|^2 + k_2 \\
&\tau_2 = w_2\phi_2 z_2, \quad w_2 > 0
\end{aligned} \qquad (10)$$

where α_{2s2} is any function satisfying the following conditions

$$\begin{aligned}
&\text{condition i} \quad z_2\left[\theta_1\alpha_{2s2} - \tilde{\theta}^T\phi_2 + \tilde{d}\right] \leq \varepsilon_2 \\
&\text{condition ii} \quad z_2\alpha_{2s2} \leq 0
\end{aligned} \qquad (11)$$

In (10) and (11), $C_{\phi 2}$ a positive definite constant diagonal matrix to be specified later, k_2 is a positive scalar, ε_2 is a positive design parameter which can be arbitrarily small, w_2 is a any positive weighting factor, and

$$\begin{aligned}
&x_{2eq} = \dot{x}_{1d} - k_p e_1, \quad \dot{x}_{2eq} = \ddot{x}_{1d} - k_p\dot{e}_1 \\
&z_2 = \dot{e}_1 + k_p e_1 = x_2 - x_{2eq} \\
&\phi_2 = \left[\alpha_{2a} - \bar{b}x_2 - \bar{F}_{fc},\ 1,\ 0,\ 0,\ 0,\ 0\right]^T
\end{aligned} \qquad (12)$$

Let $z_3 = P_L - \alpha_2$ denote the input discrepancy. For the positive semi-definite (p.s.d.) function V_2 defined by $V_2 = 1/2 w_2 z_2^2$, it can be shown that

$$\begin{aligned}
\dot{V}_2 = \ & w_2\theta_1 z_2 z_3 + w_2 z_2(\theta_1\alpha_{2s2} - \tilde{\theta}^T\phi_2 + \tilde{d}) \\
& - w_2\tfrac{\theta_1}{\theta_{1min}} k_{2s1} z_2^2
\end{aligned} \qquad (13)$$

Step 2

In Step 1, as seen from (13), if $z_3 = 0$, then, output tracking can be achieved in viewing i of (11). So Step 2 is to synthesize a virtual control function so that z_3 converges to zero or a small value with a guaranteed transient performance as follows. From (6) and (10),

$$\begin{aligned}
\dot{z}_3 = \dot{P}_L - \dot{\alpha}_2 = \ & \theta_3[-(\bar{A}_1 h_1 + \bar{A}_2\bar{A}_c h_2)x_2 \\
& + (h_1 g_3 + \bar{A}_c h_2 g_4)u] - \theta_4(x_3 - x_4)(h_1 + \bar{A}_c h_2) \\
& - \theta_5 h_1(x_3 - \bar{P}_r) + \theta_6\bar{A}_c h_2(x_4 - \bar{P}_r) - \dot{\alpha}_{2c} - \dot{\alpha}_{2u}
\end{aligned} \qquad (14)$$

where

$$\begin{aligned}
&\dot{\alpha}_{2c} = \tfrac{\partial\alpha_2}{\partial x_1}\dot{x}_2 + \tfrac{\partial\alpha_2}{\partial x_2}\hat{\dot{x}}_2 + \tfrac{\partial\alpha_2}{\partial t} \\
&\dot{\alpha}_{2u} = \tfrac{\partial\alpha_2}{\partial x_2}[-(x_3 - \bar{A}_c x_4 - \bar{b}x_2 - \bar{F}_{fc})\tilde{\theta}_1 - \tilde{\theta}_2 + \tilde{d}] + \tfrac{\partial\alpha_2}{\partial\hat{\theta}}\dot{\hat{\theta}}
\end{aligned} \qquad (15)$$

in which $\dot{\alpha}_{2c}$ is the calculable part of $\dot{\alpha}_2$ while $\dot{\alpha}_{2u}$ is the incalculable part and has to be dealt with via certain robust feedback. Define a new virtual control input Q_L as $Q_L = (h_1 g_3 + \bar{A}_c h_2 g_4)u$. Then, it is ready to see that (14) has the same form as those studied in the previously proposed ARC control designs [13] and the same design strategy can be applied to construct a virtual control law $\alpha_3(x_1, x_2, x_3, x_4, \hat{\theta}, t)$ for Q_L. The resulting control function α_3 and adaptation function $\tau_3(x_1, x_2, x_3, x_4, \hat{\theta}, t)$ are given by

$$\begin{aligned}
&\alpha_3 = \alpha_{3a} + \alpha_{3s} \\
&\quad \alpha_{3a} = -\tfrac{1}{\hat{\theta}_3}\left[\tfrac{w_2}{w_3} z_2\hat{\theta}_1 - \hat{\theta}_3(\bar{A}_1 h_1 + \bar{A}_2 h_2\bar{A}_c)x_2\right. \\
&\qquad -\hat{\theta}_4(h_1 + \bar{A}_c h_2)(x_3 - x_4) - \hat{\theta}_5 h_1(x_3 - \bar{P}_r) \\
&\qquad \left. +\hat{\theta}_6\bar{A}_c h_2(x_4 - \bar{P}_r) - \dot{\alpha}_{2c}\right] \\
&\quad \alpha_{3s} = \alpha_{3s1} + \alpha_{3s2}, \quad \alpha_{3s1} = -\tfrac{1}{\theta_{3min}} k_{3s1} z_3 \\
&\qquad k_{3s1} \geq k_3 + \|\tfrac{\partial\alpha_2}{\partial\hat{\theta}} C_{\theta 3}\|^2 + \|C_{\phi 3}\Gamma\phi_3\|^2 \\
&\tau_3 = \tau_2 + w_3\phi_3 z_3
\end{aligned} \qquad (16)$$

where w_3 is a positive weighting factor, $k_3 > 0$ is a constant, $C_{\theta 3}$, and $C_{\phi 3}$ are positive definite (p.d.) constant diagonal matrices, and α_{3s2} is a robust control function satisfying the following two conditions

$$\begin{aligned}
&\text{condition i} \quad z_3\left[\theta_3\alpha_{3s2} - \tilde{\theta}^T\phi_3 - \tfrac{\partial\alpha_2}{\partial x_2}\tilde{d}\right] \leq \varepsilon_3 \\
&\text{condition ii} \quad z_3\alpha_{3s2} \leq 0
\end{aligned} \qquad (17)$$

in which ε_3 is a positive design parameter, and

$$\phi_3 = \begin{bmatrix}
\frac{w_2}{w_3} z_2 - \frac{\partial\alpha_2}{\partial x_2}(x_3 - \bar{A}_c x_4 - \bar{b}x_2 - \bar{F}_{fc}) \\
-\frac{\partial\alpha_2}{\partial x_2} \\
-(\bar{A}_1 h_1 + \bar{A}_2\bar{A}_c h_2)x_2 + \alpha_{3a} \\
-(h_1 + \bar{A}_c h_2)(x_3 - x_4) \\
-h_1(x_3 - \bar{P}_r) \\
\bar{A}_c h_2(x_4 - \bar{P}_r)
\end{bmatrix} \qquad (18)$$

Theorem 1 *Let $\tau = \tau_3$ and determine the control input u from the following one-one continuous mapping between u and α_3*

$$\alpha_3 = [h_1(x_1)g_3(x_3, sign(u)) + \bar{A}_c h_2(x_1)g_4(x_3, sign(u))]u \qquad (19)$$

with α_3 calculated from (16). If the controller parameters $C_{\theta 3} = diag\{c_{\theta 3l}, l = 1, \ldots 6\}$, and $C_{\phi k} = diag\{c_{\phi kl}\}, k = 2, 3$ in (10) and (16) are chosen such that $c_{\phi kl}^2 \geq \frac{w_k w_3}{2c_{\theta 3l}^2}$, $\forall k, l$, then, the control law (19) with the adaptation law (8) guarantees that

A. *In general, output tracking error e_1 and $z = [z_2, z_3]^T$ are bounded. Furthermore, the p.d. function V given by $V = V_2 + \frac{1}{2}w_3 z_3^2$ is bounded above by*

$$V(t) \leq exp(-\lambda_V t)V(0) + \tfrac{\varepsilon_V}{\lambda_V}[1 - exp(-\lambda_V t)] \qquad (20)$$

where $\lambda_V = 2min\{k_2, k_3\}$ and $\varepsilon_V = w_2\varepsilon_2 + w_3\varepsilon_3$.

B. *If after a finite time t_0, $\tilde{d} = 0$, i.e., in the presence of parametric uncertainties only, then, in addition to results in A, asymptotic output tracking (or zero final tracking error) is also achieved.* Δ

Proof. The Theorem can be proved in the same way as in [13]. $\square$.

4 Comparative Experimental Results

Experiment Setup

To test the proposed nonlinear ARC strategy and study fundamental problems associated with the control of electro-hydraulic systems, a three-link robot arm (a scaled down version of excavator arm) driven by three hydraulic cylinders has been set up at the Ray W. Herrick Laboratory of the School of Mechanical Engineering. The three hydraulic cylinders are controlled by two proportional directional control valves and one servo valve manufactured by Parker Hannifan company. Currently, experiments are performed on the swing motion control of the arm (or the first joint) with the other two joints fixed. The schematic of the system is shown in Fig.2. The swing circuit is driven by a single-rod cylinder (Parker D2HXTS23A) and controlled by a servovalve (Parker BD760AAAN10). The cylinder has a built-in LVDT sensor, which provides the position and velocity information of the cylinder movement. The analog LVDT position signal has a measurement noise level equivalent to 1mm. Since the range of the velocity provided by the LVDT sensor is too small, backward difference plus filter is used to obtain the needed velocity information at high speed movement. Pressure sensors have been installed at all ports to provide the needed pressure feedback signals. All analog measurement signals (the cylinder position, velocity, forward and return chamber pressures, and the supplied pressure) are fed back to a Pentium PC through a plugged in A/D and D/A board.

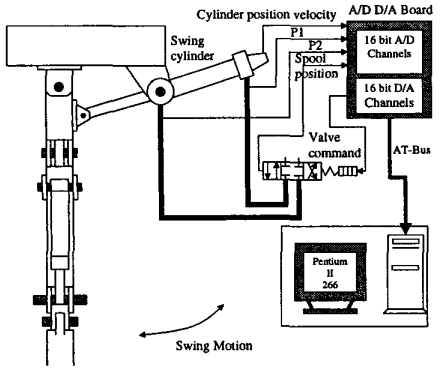

Figure 2: Schematic of Experimental Setup

System Identification

For the swing motion shown in Fig.2, due to the nonlinear transformation between the joint swing angle q and the cylinder position x_L, the equivalent mass m of a constant swing inertia seeing at the swing cylinder coordinate depends on the swing angle or the cylinder position x_L as well. However, by restricting the movement of the swing cylinder in its middle range, this equivalent mass m will not change much and thus can be treated as constant, which is around $2200kg$ for the no load situation. Although tests have been done to identify the friction curve, for simplicity, it is not used in the following experiments (i.e., $b = F_{fc} = 0$ in 1) to test the robustness of the proposed algorithm to these *hard-to-model* terms. The cylinder physical parameters are $A_1 = 3.1416in^2$, $A_2 = 1.6567in^2$, $V_{h1} = 30.48in^3$, and $V_{h2} = 55.33in^3$. By assuming no leakage flows and moving the cylinder at different constant velocities, we can back out the flow mapping of the servovalve. The estimated flow gains are $k_{q1} = 0.1820in^3/(\sqrt{psi}secV)$ and $k_{q2} = 0.1886in^3/(\sqrt{psi}secV)$. Dynamic tests are also performed and reveal that the servovalve has a bandwidth around 10Hz. The effective bulk modulus is estimated around $2.71 \times 10^8 Pa$.

Control Algorithms

Three controllers are tested for comparison:

ARC : the controller proposed in this paper and described in previous sections. For simplicity, in the experiments, only two parameters, θ_1, and θ_2, are adapted; the first parameter represents the effect of the equivalent mass and the second parameter represents the effect of the nominal value of the lumped disturbance. Since the valve dynamics is neglected and its bandwidth is not so high (around 10Hz), not so large feedback gains are used to avoid instability; the control gains used are $k_p = k_2 = k_3 = 19$. The scaling factors of $s_{c3} = 2.8085 \times 10^6$ and $s_{c4} = 0.08588$, are used. Adaptation rates are set at $\Gamma = diag\{0.01, 0.08\}$.

DRC : the same control law as ARC but without using parameter adaptation, i.e., letting $\Gamma = diag\{0, 0\}$. In such a case, the proposed ARC control law becomes a deterministic robust control law [11].

Motion Controller : the state-of-the-art industrial motion controller bought from Parker Hannifian company (Parker's PMC6270ANI 2-axis motion controller) along with the Parker's cylinder and valves used for the experiments. Controller gains are obtained by strictly following the gain tuning process stated in the "Servo Tuner User Guide" coming with the motion controller [15]. The tuned gains are $SGP = 20, SGI = 0.5, SGV = 22, SGVF = 100, SGAF = 0.02$. The controller is essentially a PID controller with velocity and acceleration feedforward.

Comparative Experimental Results

The three controllers are first tested for a slow point-to-point motion trajectory shown in Fig.3, which has a maximum velocity of $v_{max} = 0.1m/sec$ and a maximum acceleration of $a_{max} = 0.2m/sec^2$. The tracking errors are shown in Fig.4. As seen, the proposed DRC and ARC have a better performance than the Motion Controller in term of both transient and final tracking errors. Due to the use of parameter adaptation, the final tracking error of ARC is almost reduced to the measurement noise level of the position sensor while DRC still has a slight offset. This illustrates the effectiveness of using parameter adaptation.

To test the performance robustness of the proposed algorithms to parameter variations, a 45kg load is added at the end of the robot arm, which increases the equivalent mass of the cylinder to $4000kg$. The tracking errors are shown in Fig.5. As seen, even for such a short one-run experiment, the adaptation algorithm of the ARC controller is able to pick up the change of the inertial load and an improved performance is achieved in comparison to the non-adaptive DRC. Again, both ARC and DRC exhibit better performance than Motion Controller.

The three controllers are then run for a fast point-point motion trajectory shown in Fig.3, which has a maximum velocity of $v_{max} = 0.3m/sec$ and an acceleration of

$a_{max} = 3m/sec^2$; both are near their physical limits. The tracking errors are shown in Fig.6. As seen, the Motion Controller cannot handle such an aggressive movement well and a large tracking error around 15-20mm exhibits during the constant high-speed movement. In contrast, the tracking error of ARC during the entire run is kept within 5mm. Furthermore, the tracking error goes back to the measurement noise level very quickly after the short large acceleration and deceleration periods. Transient pressure and control input plots (not shown) reveal that the system is actually at its full capacity during the short large acceleration and deceleration periods.

Experiments are also run for other point-point motion with different velocity limits and for sinusoidal desired trajectories with different frequencies. In all those tests, the same trend as in above runs can be concluded. All these results show the excellent tracking capability of the proposed nonlinear ARC algorithm in spite of parameter variations and model uncertainties. It is worth noting that the proposed controller reduces tracking errors almost down to measurement resolution level except during high acceleration and deceleration periods.

ACKNOELEGMENT

This work is supported in part by the National Science Foundation under the CAREER grant CMS-9734345

References

[1] H. E. Merritt, *Hydraulic control systems*. New York: Wiley, 1967.

[2] T. C. Tsao and M. Tomizuka, "Robust adaptive and repetitive digital control and application to hydraulic servo for noncircular machining," *ASME J. Dynamic Systems, Measurement, and Control*, vol. 116, pp. 24–32, 1994.

[3] P. M. FitzSimons and J. J. Palazzolo, "Part i: Modeling of a one-degree-of-freedom active hydraulic mount; part ii: Control," *ASME J. Dynamic Systems, Measurement, and Control*, vol. 118, no. 4, pp. 439–448, 1996.

[4] A. R. Plummer and N. D. Vaughan, "Robust adaptive control for hydraulic servosystems," *ASME J. Dynamic System, Measurement and Control*, vol. 118, pp. 237–244, 1996.

[5] J. E. Bobrow and K. Lum, "Adaptive, high bandwidth control of a hydraulic actuator," *ASME J. Dynamic Systems, Measurement, and Control*, vol. 118, pp. 714–720, 1996.

[6] R. Vossoughi and M. Donath, "Dynamic feedback linearization for electro-hydraulically actuated control systems," *ASME J. Dynamic Systems, Measurement, and Control*, vol. 117, no. 4, pp. 468–477, 1995.

[7] L. D. Re and A. Isidori, "Performance enhancement of nonlinear drives by feedback linearization of linear-bilinear cascade models," *IEEE Trans. on Control Systems Technology*, vol. 3, no. 3, pp. 299–308, 1995.

[8] A. Alleyne and J. K. Hedrick, "Nonlinear adaptive control of active suspension," *IEEE Trans. on Control Systems Technology*, vol. 3, no. 1, pp. 94–101, 1995.

[9] B. Yao, G. T. C. Chiu, and J. T. Reedy, "Nonlinear adaptive robust control of one-dof electro-hydraulic servo systems," in *ASME International Mechanical Engineering Congress and Exposition (IMECE'97), FPST-Vol.4*, (Dallas), pp. 191–197, 1997.

[10] B. Yao and M. Tomizuka, "Smooth robust adaptive sliding mode control of robot manipulators with guaranteed transient performance," in *Proc. of American Control Conference*, pp. 1176–1180, 1994. The full paper appeared in *ASME Journal of Dynamic Systems, Measurement and Control*, Vol. 118, No.4, pp764-775, 1996.

[11] B. Yao, "High performance adaptive robust control of nonlinear systems: a general framework and new schemes," in *Proc. of IEEE Conference on Decision and Control*, pp. 2489–2494, 1997.

[12] B. Yao and M. Tomizuka, "Adaptive robust control of siso nonlinear systems in a semi-strict feedback form," *Automatica*, vol. 33, no. 5, pp. 893–900, 1997. (Part of the paper appeared in Proc. of 1995 American Control Conference, pp2500-2505).

[13] B. Yao, F. Bu, and G. T. C. Chiu, "Nonlinear adaptive robust control of electro-hydraulic servo systems with discontinuous projections," in *Proc. of IEEE Conf. on Decision and Control*, pp. 2265–2270, 1998.

[14] B. Yao, M. Al-Majed, and M. Tomizuka, "High performance robust motion control of machine tools: An adaptive robust control approach and comparative experiments," *IEEE/ASME Trans. on Mechatronics*, vol. 2, no. 2, pp. 63–76, 1997. (Part of the paper also appeared in *Proc. of 1997 American Control Conference*).

[15] C. D. P. H. Co., *Servo tuner user guide*. Software Mannual, Nov. 1994.

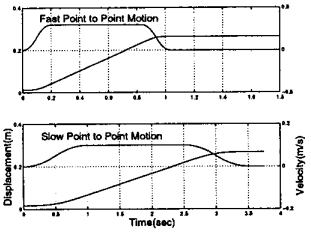

Figure 3: Point-to-point motion trajectory

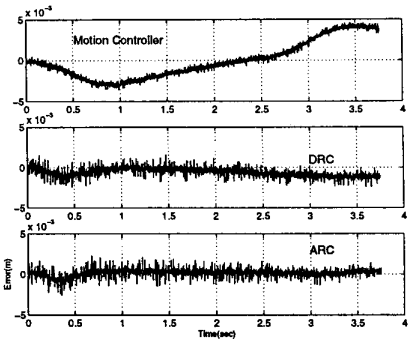

Figure 4: Tracking errors for the slow point-to-point motion without load

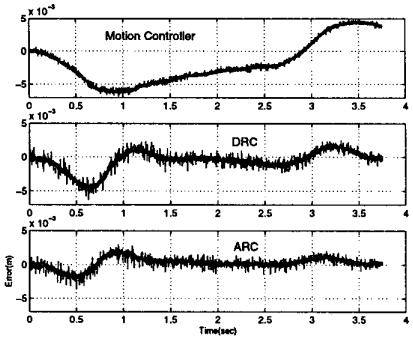

Figure 5: Tracking errors for the slow point-to-point motion with load

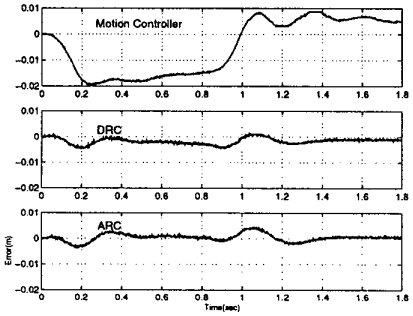

Figure 6: Tracking errors for the fast point-to-point motion without load